

Star formation history of early-type galaxies in low density environments.

IV. What do we learn from nuclear line-strength indices?

M. Longhetti¹, A. Bressan², C. Chiosi^{3*}, R. Rampazzo⁴

¹Institut d'Astrophysique, 98 bis Boulevard Arago, 75014 Paris, France

²Osservatorio Astronomico di Padova, Vicolo dell'Osservatorio, 5, 35122 Padova, Italy

³Dipartimento di Astronomia, Università di Padova, Vicolo dell'Osservatorio, 5, 35122 Padova, Italy

⁴Osservatorio Astronomico di Brera, Via Brera 28, 20121 Milano, Italy

Received 8 March 1999; Accepted 31 August 1999

Abstract. In this paper we analyze the line-strength indices in the Lick-system measured by Longhetti et al. (1998a, b) for a sample of 51 early-type galaxies located in low density environments (LDE) and showing signatures of fine structures and/or interactions. The sample contains 21 shell-galaxies and 30 members of interacting pairs.

Firstly we perform a preliminary comparison between three different sources of calibrations of the line strength indices, namely Buzzoni et al. (1992, 1994), Worthey (1992), Worthey et al. (1994) and Idiart et al. (1995), derived from stars with different effective temperature, gravity, and metallicity. Looking at the three indices in common, i.e. Mg2, Fe5270, and H β , the calibrations by Buzzoni et al. (1992, 1994), Worthey (1992) and Worthey et al. (1994) lead to mutually consistent results. The calibration of H β by Idiart et al. (1995) can be compared with the previous ones only for a limited range of ages, in which good agreement is found. Mg2 and Mgb indices predicted by the Idiart's et al. (1995) fitting functions result to be systematically lower than those obtained from using Worthey (1992) calibrations.

Secondly, we discuss the properties of the galaxies in our sample by comparing them both with theoretical Single Stellar Populations (SSPs) and the *normal* galaxies of the González (1993: G93) sample. The analysis is performed by means of several diagnostic planes.

In the σ , Mg2, Fe5270 and Fe5335 space, *normal*, shell- and pair-galaxies have a different behavior. First of all, normal and pair-galaxies follow the universal σ vs. Mg2 relation, whereas shell-galaxies lie above it; secondly the Fe versus Mg2 relation of normal, shell- and pair-galaxies is flatter than the theoretical expectation. This fact hints for enhancement of α -elements with respect to solar parti-

tion in galaxies with strong Fe indices and/or high velocity dispersion, mass and luminosity in turn.

In the σ vs. H β plane *normal* galaxies seem to follow a nice relation suggesting that objects with shallow gravitational potential have strong H β values (youth signature?), whereas shell- and pair-galaxies scatter all over the plane. A group of galaxies with deep gravitational potential and strong H β is found. Is this a signature of recent star formation?

In the H β vs. [MgFe] plane, ¹ which is perhaps best suited to infer the age of the stellar populations, the peculiar galaxies in our sample show nearly the same distribution of the *normal* galaxies in the G93 sample. There is however a number of peculiar galaxies with much stronger H β . Does this mean that the scatter in the H β vs. [MgFe] plane, of normal, shell- and pair-galaxies has a common origin, perhaps a secondary episode of star formation? We suggest that, owing to their apparent *youth*, shell- and pair-galaxies should have experienced at least one interaction event after their formation. The explanation comes natural for shell- and pair-galaxies where the signatures of interactions are evident. It is more intriguing in *normal* galaxies (perhaps other causes may concur).

Noteworthy, the distribution in the H β vs. [MgFe] plane of *normal*, shell- and pair-galaxies is confined within a narrow strip that runs significantly steeper than the path followed by aging SSPs. This feature is explained as due to metal enrichment always accompanying star formation.

Shell-galaxies encompass the whole range of ages inferred from the H β vs. [MgFe] plane, indicating that among them recent and old interaction/acquisition events are equally probable. If shells are formed at the same time at which the rejuvenating event took place, shells ought to be long lasting phenomena.

Send offprint requests to: M. Longhetti

* Visiting Scientist, Max-Planck Institut für Astrophysik, K-Schwarzschild str. 1, D-87540, Garching bei München, Germany

¹ $[MgFe] = \sqrt{\langle Fe \rangle \times Mgb}$,
 $\langle Fe \rangle = (Fe5270 + Fe5335)/2$

Key words: Galaxies: elliptical and lenticular, cD; Galaxies: evolution; Galaxies: formation; Galaxies: fundamental parameters; Galaxies: interactions; Galaxies: star-bursts

1. Introduction

Hierarchical clustering scenarios predict that early-type galaxies we see today in large virialized structures and in low density environments have formed at different epochs (Ellis 1998 and references therein). Cluster objects formed through major merging events at red-shift $z > 3$, whereas early-type galaxies, today at the border of large structures, have formed significantly later, at $z < 1$.

The morphology of early-type galaxies shows many relationships of different kind with the surrounding environment. The population of the early-type galaxies in clusters appears to be homogeneous contrary-wise to the large heterogeneity shown by objects inhabiting the low density media. Although the bulk of galaxies visible today in low density environments are already in place at $z \approx 0.5$ (Griffith et al. 1994), i.e. nearly half the Hubble time, a large number of them show peculiarities such as signatures of interaction, fine structures etc. (see Schweizer 1992; Reduzzi et al. 1996 and references therein) which may hint at more recent activity.

In the above framework, early-type galaxies are currently interpreted as the final product of major/minor merging events (Schweizer 1992; Barnes 1996). Nevertheless, both from observational and theoretical points of view, evidence has grown over the years that different mechanisms have also played a significant role in shaping their final structure. In clusters, galaxy encounters are fast enough to make mergers less probable than *harassments* (Moore et al. 1996). In low density environments encounters are most likely to result in a merger (Barnes & Hernquist 1992) but dissipative mechanisms (Bender 1997) and *weak-interaction* events (Thomson 1991) could also contribute to the structural evolution of a galaxy.

This paper is the fourth of a series dedicated to the study of typical galaxies in low density environments, i.e. galaxies showing signatures of present/past interactions. The sample is composed of 21 shell-galaxies and 30 members of interacting pairs most of which show fine structures. Among them shell-galaxies represent a class of objects exhibiting signatures of past interactions, i.e. minor/major mergers (Schweizer 1992) or weak-interactions (Thomson & Wright 1990) and Thomson (1991). Pair-members are instead objects with ongoing interaction.

Longhetti et al. (1998a) measured 19 line-strength indices in the nuclear regions of the galaxies in our sample. Sixteen indices belong to the group defined by Worthey (1992) and G93 and include $H\beta$, Mg2 and some Fe features. All indices were transformed into the Lick-IDS system. Furthermore, three indices, particularly sensitive to recent star formation (Rose 1984, 1985; Leonardi & Rose

1996), i. e. $\Delta 4000$, $H\delta/FeI$ and $CaII(H+K)$, were added to the list. Longhetti et al. (1998b) derived the inner kinematics of the sample and corrected the line-strength indices for central velocity dispersion (Longhetti et al. 1998a).

The comparison of these galaxies with those in Virgo and Fornax (Rampazzo et al. 1999a) singled out a group of pair-galaxies in our sample with peculiar behavior in the $(\log R_e, \mu_e)$ plane and the κ space. These galaxies, apparently missing among cluster early-type objects, are tidally stretched and most likely in early stages of interaction. This finding makes evident the large scatter of line-strength indices as compared to galaxy scale properties. As an example, the correlation between galaxy shapes (as measured by the $a4/a$ parameter) and ages (as deduced from $H\beta$) that was advanced by de Jong & Davies (1997) is not confirmed by the Rampazzo et al. (1999a,b) study.

The purpose of this paper is to cast light on the past star formation (SF) history of shell- and pair-galaxies in LDE as traced by their line strength indices, with particular attention to the role played by dynamical interactions in triggering star formation. The comparison with the results obtained for galaxies in denser environments (Burstein et al. 1984; Pickles 1985; Rose 1995; Bower et al. 1990; G93) will help us to understand the effects of the environment on the formation/evolution of early-type galaxies.

In addition to this, we address the problem of the origin of shell structures by analyzing the evolutionary history of the stellar populations hosted by the nucleus of the interacting galaxy. Numerical simulations of dynamical interactions among galaxies yield still contrasting explanations for the occurrence of shells (Weil & Hernquist 1993; Thomson 1991). In this study, we seek to assess the duration of the shell phenomenon by means of the age of the last episode of star formation as inferred from the nuclear indices.

The paper is organized as follows. In Sect. 2 we compare indices for Single Stellar Populations (SSPs) obtained using *fitting functions* by different authors (Buzzoni et al. 1992, 1994; Worthey 1992; Idiart et al. 1995) and a unique source of isochrones (Bertelli et al. 1994). By doing so, we are able to quantify the uncertainties affecting line strength indices calculations. Based on this preliminary comparison, we adopt the fitting functions of Worthey (1992). In Sect. 3 we introduce the sample of galaxies of G93 adopted as the reference template. In Sect. 4, firstly we compare the observational line strength indices for the nuclear region of galaxies in our sample with the theoretical predictions, and secondly we compare our sample of shell- and pair-galaxies with that of *normal* elliptical galaxies by G93. Notes on individual galaxies in the $H\beta$ vs. $[MgFe]$ diagram are reported in Sect. 5. A tentative explanation of the distribution of galaxies in the $H\beta$ vs. $[MgFe]$ diagram is presented in Sect. 6 both for the present sample and the template. The interpretation is based on

Table 1. Comparison between SSP indices derived from different fitting functions

	$\Delta\%$	$\sqrt{\Delta^2\%}$	$\Delta\%$	$\sqrt{\Delta^2\%}$	$\Delta\%$	$\sqrt{\Delta^2\%}$	$\Delta\%$	$\sqrt{\Delta^2\%}$	$\Delta\%$	$\sqrt{\Delta^2\%}$
			T>3Gyr	T>3Gyr	T<3Gyr	T<3Gyr	T>1Gyr	T>1Gyr	T<1Gyr	T<1Gyr
Worthey - Idiart										
H β			-34.72	40.36						
Mg2	12.72	12.94	9.45	9.45	22.97	23.53	10.31	10.32	27.28	6.92
Mgb	15.50	15.76	11.19	11.23	29.17	29.87	12.39	12.44	34.65	8.76
Worthey - Buzzoni										
H β	-6.34	11.19	-4.29	4.75	-6.99	10.31	-2.51	3.85	-8.40	2.64
Mg2	96.88	168.29	-1.82	3.20	-837.16	-1006.74	2.75	11.27	-386.13	-107.19
Fe5270	36.49	76.69	-7.89	8.21	284.63	354.45	-5.11	9.09	1837.04	520.67
Fe5335	6.52	10.54	-0.80	2.65	24.30	24.74	0.39	5.79	28.63	29.23

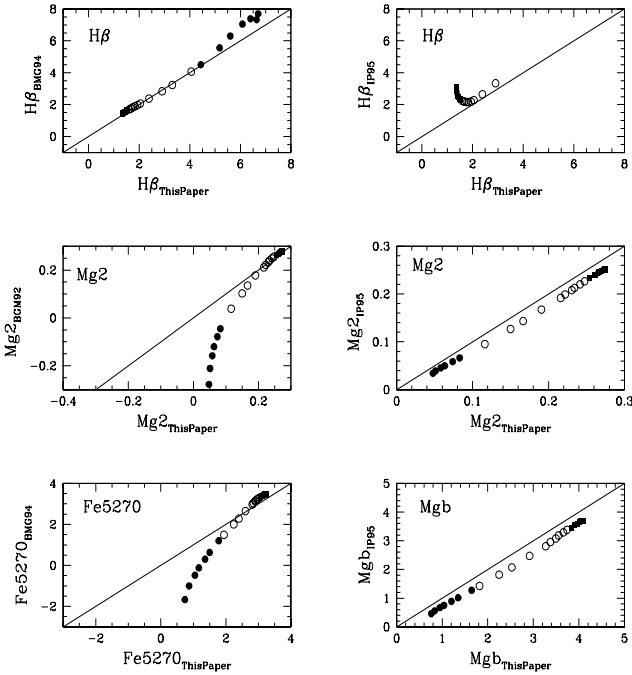


Fig. 1. Comparison between indices derived from the Lick-system fitting functions (adopted in this paper) and those from Buzzoni et al. (1992, 1994; shortly indicated by BGM92 and BMG94 respectively) and Idiart et al. (1995; IP95). In the case of Buzzoni et al. (1992, 1994) we compare the indices H β , Mg2 and Fe5270. In the case of Idiart et al. (1995) we examine the indices H β , Mg2 and Mgb. The data refer to SSPs with solar metallicity ($Z = 0.02$) and different ages: full circles for ages between 0.2 and 0.9 Gyr; open circles for ages between 1 and 9; full squares for ages between 10 and 19 Gyr.

statistical simulations of the observations. Finally, Sect. 7 summarizes the results.

2. Line-strength indices for SSPs

The technique to calculate line-strength indices of SSPs is amply described in Worthey (1994), Bressan et al. (1996) and Tantalo et al. (1998). The latter improved their previous models by introducing a differential method particularly suited to understand the role of the three main parameters driving the strength of selected indices, namely age, metallicity and enhancement in the abundance of α elements with respect to the solar partition. The reader is referred to those articles and references therein for a detailed description of the method. Here we limit ourselves to summarize a few basic properties of the models in usage. The galaxy indices are based on the isochrones of Bertelli et al. (1994), which provide the relative number of stars per elemental area of the Hertzsprung-Russell Diagram (HRD), the atlas of theoretical stellar spectra by Kurucz (1992), which is used to calculate the energy distribution in the continuum of each pass-band of interest, and a set of fitting functions.

The elemental areas of the HRD along the path drawn by an isochrone are taken sufficiently small so that all stars in each of them have the same effective temperature, gravity, luminosity and chemical composition.

The Kurucz (1992) library is extended at high temperatures by black-bodies and at temperatures cooler than 3500° K (late K and M type) by implementing the libraries of Lancon & Rocca-Volmerange (1992), Straizys & Sviderskiene (1972), and Fluks et al. (1994), see Bressan et al. (1994) and Tantalo et al. (1996) for all the details.

The *fitting functions* depend on stellar effective temperature, gravity and metallicity. They are used to calculate the line strength indices for each elemental area of the HRD. Finally a suitable integration technique yields the total indices for each SSP (isochrone).

Direct measurements of line strength indices on the integrated spectral energy distribution of individual SSPs is not possible, because the Kurucz (1992) library contains spectra at low resolution. A different strategy would be to replace this library with another one containing medium

Table 2. SSP indices obtained adopting the Lick fitting functions

Z=0.004						
Age	H β	Mg2	Mgb	Fe52	Fe53	MgFe
7.70	5.10	-0.57	0.44	0.64	0.44	0.49
7.85	5.51	-0.58	0.45	0.52	0.33	0.44
8.00	5.72	-0.56	0.49	0.48	0.28	0.43
8.95	5.09	0.06	0.97	0.83	0.61	0.84
9.00	4.82	0.06	1.05	0.93	0.71	0.93
9.18	4.01	0.08	1.27	1.27	0.96	1.19
9.70	2.41	0.12	1.94	1.77	1.47	1.77
9.78	2.27	0.13	2.03	1.83	1.53	1.85
9.85	2.14	0.13	2.12	1.89	1.59	1.92
9.90	2.02	0.14	2.19	1.95	1.64	1.98
9.95	1.98	0.14	2.24	1.95	1.65	2.01
10.00	1.91	0.14	2.28	1.99	1.69	2.05
10.04	1.84	0.15	2.33	2.02	1.74	2.09
10.08	1.78	0.15	2.37	2.06	1.78	2.14
10.18	1.71	0.15	2.42	2.06	1.81	2.16
Z=0.02						
7.70	5.25	0.06	0.61	0.88	0.91	0.74
7.85	5.65	0.05	0.65	0.84	0.87	0.75
8.00	6.00	0.05	0.73	0.81	0.86	0.78
8.95	4.44	0.10	1.65	1.78	1.54	1.65
9.00	4.06	0.12	1.82	1.94	1.69	1.82
9.18	3.31	0.15	2.25	2.24	1.99	2.18
9.70	1.94	0.22	3.37	2.84	2.54	3.01
9.78	1.83	0.23	3.49	2.90	2.60	3.10
9.85	1.76	0.23	3.56	2.92	2.61	3.14
9.90	1.68	0.24	3.66	2.97	2.66	3.21
9.95	1.61	0.25	3.74	3.02	2.71	3.27
10.00	1.54	0.25	3.83	3.07	2.75	3.34
10.04	1.49	0.26	3.91	3.12	2.80	3.40
10.08	1.45	0.26	3.96	3.15	2.83	3.44
10.18	1.37	0.27	4.08	3.21	2.89	3.53
Z=0.05						
7.70	6.21	0.06	0.75	0.85	1.14	0.86
7.85	6.46	0.06	0.75	0.92	1.21	0.90
8.00	6.74	0.06	0.75	0.96	1.25	0.91
8.95	3.81	0.16	2.30	2.57	2.36	2.38
9.00	3.50	0.17	2.50	2.71	2.48	2.55
9.18	2.79	0.21	3.02	3.03	2.78	2.96
9.70	1.70	0.30	4.34	3.60	3.31	3.87
9.78	1.60	0.31	4.51	3.67	3.38	3.99
9.85	1.50	0.33	4.67	3.75	3.47	4.11
9.90	1.47	0.33	4.72	3.76	3.47	4.13
9.95	1.41	0.34	4.84	3.81	3.52	4.21
10.00	1.36	0.34	4.94	3.86	3.57	4.28
10.04	1.34	0.35	4.95	3.87	3.58	4.29
10.08	1.32	0.35	4.99	3.88	3.58	4.32
10.18	1.24	0.36	5.09	3.96	3.66	4.41

resolution spectra on which the direct measurement of the indices could be made. This possibility, explored in a forthcoming paper, is no longer considered here.

2.1. Uncertainties on the line-strength indices

In this section we compare line-strength indices computed by adopting fitting functions from different authors, namely Worthey (1992) and Worthey et al. (1994), oth-

erwise known as the Lick-system, Buzzoni et al. (1992, 1994), and Idiart et al. (1995).

The Lick fitting functions refer to 21 line-strength indices (Worthey 1992; Gorgas et al. 1993; Worthey et al. 1994) and are based on a library of stellar spectra containing about 400 stars, observed at the Lick Observatory between 1972 and 1984, with an Image Dissector Scanner (IDS). In the following we adopt the Worthey (1992) fitting functions, extended however to high temperature stars ($T_{eff} \approx 10000^{\circ}\text{K}$) as reported in Longhetti et al. (1998a).

The Buzzoni et al. (1992) fitting functions for the Mg2, Fe5270 and H β indices, rest on a library of spectra for 74 stars. Buzzoni et al. (1994) do not consider the dependence of the H β on the metallicity.

Idiart et al. (1995) present calibrations for Mg2, Mgb and H β , based on a library of 170 stars, among which 89 are new observations, and the remaining are from Faber et al. (1985) and Gorgas et al. (1993) data. The sample spans the metallicity range $-3.0 < [\text{Fe}/\text{H}] < 0.2$, the gravity range $0.7 < \log(g) < 5.0$ and the temperature range $3800^{\circ}\text{K} < T_{eff} < 6500^{\circ}\text{K}$.

We construct integrated narrow band indices for SSPs of solar metallicity by applying the different fitting functions above to the same set of stellar isochrones. This allows us to single out the effects of different empirical relations and evaluate the corresponding uncertainty.

The comparison between the three different sets of models for the indices in common is shown in Fig. 1.

Good agreement between Worthey (1992) and Buzzoni et al. (1992, 1994) calibrations exists for the H β index of SSPs older than 1 Gyr, where the mean difference between the two sources is $\approx 2\%$ (see Table 1). For SSPs younger than 1 Gyr the fitting functions by Buzzoni et al. (1992, 1994) slightly overestimate the index H β with respect to those by Worthey (1992). Furthermore, the Mg2 and Fe5270 indices, more sensitive to changes in metallicity, agree only for SSPs older than 3 Gyr. For younger SSPs, they differ by large factors. It is worth recalling that Buzzoni et al. (1992, 1994) considered their calibration to be applicable only to old SSPs.

The calibrations by Idiart et al. (1995) fit the behavior of Mg2, Mgb and H β for stellar temperatures between 3800 K and 6500 K. The features measured by the Mg2 and Mgb indices are strongly dominated by relatively cool stars, both in young and old SSPs. On the contrary, the H β index mainly reflects the contribution of main sequence and turn off stars of a stellar population.

Unfortunately, at ages younger than 2 Gyr the effective temperatures of these stars are higher than 6500 K, the upper limit of those fitting functions (Bertelli et al 1994). Therefore, values obtained for the H β index adopting the calibration of Idiart et al. (1995) are reliable only for relatively old SSPs. Indeed, when only SSPs older than 2 Gyr are compared, good agreement between Idiart's et al. (1995) and Worthey's et al. (1994) calibration of H β

is found (see Fig. 1). In contrast, for ages older than 10 Gyr, the effect of main sequence stars cooler than 3800 K (for which the index has been extrapolated out of the range of validity of the calibrations) can be seen in the growing disagreement between the predictions of Idiart et al. (1995) and those of the Lick system.

The predictions for Mg2 and Mgb do not suffer from this limitation in temperature, therefore they can be extended also to young SSPs as shown in Fig. 1. The Mg2 and Mgb indices derived from Idiart's et al. (1995) fitting functions are systematically lower than those from Worthey (1992) calibrations, with an offset of 0.02 mag for Mg2 and 0.36 mag for Mgb. These systematic shifts are probably due to the different sample of stars adopted by Idiart et al. (1995), that leads to a different calibration of the indices with respect to the stellar gravity.

In Table 1 we present the detailed comparison of results obtained from using Worthey (1992), Buzzoni et al. (1992, 1994), and Idiart et al. (1995): Table 1 lists $\Delta\%$ (average difference between the two sets of indices values) and $\sqrt{\Delta^2}\%$ (root square of the average quadratic difference) for different values of the age as indicated.

In the following we will adopt Worthey (1992) as the reference calibration, and consider the average offset between Buzzoni et al. (1992) and Worthey (1992) predictions, as representative of the uncertainty of the models. Indices calculated with this set of fitting functions are reported in Table 2 for three different metallicities, and for ages between 5×10^7 yr and 15 Gyr.

3. Remarks on the observational data

3.1. The reference sample by G93

G93 obtained long-slit spectroscopic data for a sample of 41 elliptical galaxies. He derived kinematic profiles and line-strength indices for the nuclear regions (within 1/8 of the effective radius) and for a wider coverage of the galaxies area (within 1/2 of the effective radius), thus providing information on the radial gradients in these quantities. G93 sample of galaxies is the reference frame to which often in the course of this paper our data will be compared. In order to make the G93 data fully consistent with our ones, we start from his raw data within the central $5''$, to which we apply the correction for velocity dispersion (see below). The corrected data are listed in Table 3.

3.2. Correcting G93 for velocity dispersion

The correction of the G93 data for velocity dispersion is made using the method of Longhetti et al. (1998a) for the sake of internal consistency. We remind the reader that G93 corrected his data for velocity dispersion, but using a different method. Although Longhetti et al. (1998b) demonstrated that good agreement exists between our kinematic parameters and those of G93, and that the dif-

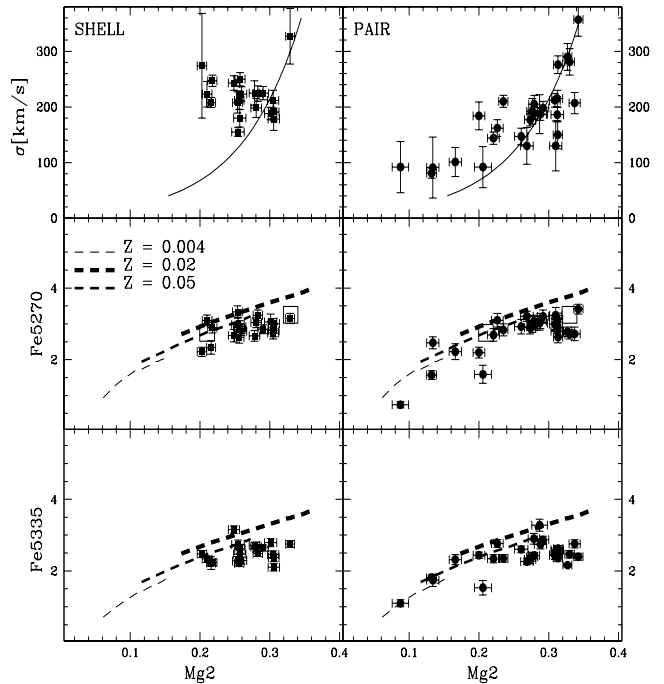


Fig. 2. Velocity dispersion σ and iron indices (Fe5270 and Fe5335) vs. Mg2 for shell- (left panels) and pair-galaxies (right panels). Lines in the upper panels represent the Mg2 - σ relation by Bender et al. (1993). The dashed lines represent the SSP models for three different metallicities, namely $Z=0.004$, $Z=0.02$ (the solar value), and $Z=0.05$ in the age range 1 to 15 Gyr (the age increases from left to right). The open squares in the Fe5270 vs. Mg2 panels represent the mean values calculated by Worthey et al. (1992) for a sample of *compact* (left) and *giant* galaxies (right)

ferences brought about by the two methods for correcting indices for velocity dispersion are statistically small, yet they may lead to systematic discrepancies between the two data sets in the $[\text{MgFe}] - \text{H}\beta$ diagram. Since our aim is to single out physical differences between *normal* (G93) and *interacting or post-interacting* galaxies, we need to clean the data for all possible effects of spurious nature.

3.3. Effects of emission lines on G93 data

Although the G93 sample was selected to exclude galaxies with large amounts of gas, a substantial fraction of the ellipticals in this list (28/40) clearly shows evidence of emission ($\text{EW} \leq 0.15\text{\AA}$) in the $[\text{OIII}](5007\text{\AA})$ line, at least in the central parts of the galaxies. Emission is not strong (only one galaxy, NGC 4278 has $[\text{OIII}](5007\text{\AA})$ emission larger than 1\AA) but it can seriously affect the interpretation of the $\text{H}\beta$ index. To cope with this difficulty, G93 tried to cure the $\text{H}\beta$ index of his galaxies for emission

Table 3. The G93 data within 5'' after correction for velocity dispersion σ (in km/s).

Name	H β	Mg2	Mgb	Fe52	Fe53	MgFe	σ	Name	H β	Mg2	Mgb	Fe52	Fe53	MgFe	σ
NGC221	2.28	0.22	2.98	3.00	2.68	3.60	77	NGC5812	1.71	0.34	4.47	2.84	2.51	4.27	200
NGC224	1.67	0.34	4.58	3.07	2.64	4.48	183	NGC5813	1.23	0.32	4.53	2.60	2.03	4.05	220
NGC315	1.00	0.32	4.21	2.37	1.84	3.72	310	NGC5831	1.83	0.30	4.31	3.06	2.60	4.33	163
NGC507	1.67	0.32	4.02	2.54	2.07	3.79	275	NGC5846	1.17	0.34	4.61	2.65	2.18	4.15	228
NGC547	1.27	0.32	4.59	2.57	1.98	4.05	242	NGC6127	1.52	0.33	4.47	2.55	2.10	4.01	245
NGC584	1.82	0.29	4.05	2.78	2.30	3.99	198	NGC6702	2.10	0.25	3.57	2.87	2.46	3.83	174
NGC636	1.86	0.28	3.96	2.97	2.48	4.08	163	NGC6703	1.63	0.29	4.10	2.82	2.36	4.05	184
NGC720	1.54	0.35	4.71	2.62	2.21	4.19	247	NGC7052	0.89	0.33	4.47	2.48	1.95	3.93	286
NGC821	1.66	0.33	4.45	2.88	2.35	4.25	196	NGC7454	2.05	0.23	3.23	2.56	2.21	3.45	103
NGC1453	0.89	0.31	4.21	2.52	1.94	3.83	294	NGC7562	1.62	0.30	4.07	2.67	2.03	3.87	244
NGC1600	1.42	0.34	4.38	2.38	2.02	3.86	325	NGC7619	1.46	0.34	4.35	2.57	2.00	3.94	314
NGC1700	1.92	0.29	3.77	2.81	2.23	3.85	226	NGC7626	1.48	0.35	4.59	2.13	2.06	3.80	259
NGC2300	1.70	0.35	4.45	2.67	2.04	4.05	264	NGC7785	1.48	0.31	4.20	2.60	2.18	3.94	239
NGC2778	1.29	0.35	4.43	2.81	2.35	4.20	157	NGC4261	1.09	0.35	4.52	2.68	1.96	4.07	305
NGC3377	1.85	0.29	4.07	2.66	2.28	3.93	126	NGC4374	1.00	0.33	4.31	2.51	1.85	3.84	289
NGC3379	1.42	0.34	4.47	2.73	2.21	4.14	212	NGC4472	1.73	0.32	4.33	2.51	2.14	3.94	290
NGC3608	1.61	0.33	4.36	2.70	2.31	4.10	187	NGC4478	1.81	0.29	4.09	2.80	2.51	4.08	127
NGC3818	1.48	0.33	4.60	2.78	2.42	4.28	174	NGC4552	1.31	0.36	4.69	2.63	2.21	4.19	256
NGC4278	-1.13	0.33	4.57	2.39	1.99	3.93	246	NGC4649	1.38	0.37	4.55	2.44	1.88	3.92	349
NGC4489	2.30	0.25	3.27	2.98	2.49	3.72	48	NGC4697	1.58	0.30	4.32	3.00	2.54	4.29	161
NGC5638	1.62	0.32	4.53	2.89	2.36	4.29	153								

contamination adopting a linear relation between the intensity of the H β emission line and that of the forbidden line [OIII](5007Å). This correlation has been found empirically, measuring the two emission lines on a sample of galaxies. However, the measure of the H β emission line is not an easy task, because of the possible contamination by the *absorption* component, and the correct evaluation of the effect of H β emission line on the H β index requires detailed models of the emission/absorption processes. Therefore, instead of applying uncertain corrections, we prefer to leave H β unchanged and always keep in mind that G93 data adopted in the present work are not corrected for this effect.

3.4. The sample of shell- and pair-galaxies

All the data in our sample refer to the central 5'' portion of the objects and therefore are homogeneous with those by G93. Nevertheless, we have checked how the indices would change when 5'' region in our data is smaller or greater than 1/8 of the effective radius. No sizable difference has been noticed, so that no correction for aperture is applied.

Furthermore, all observational indices have been corrected for velocity dispersion (σ). This strictly follows the same procedure as in Longhetti et al. (1998a) so that no details are given here.

Finally, Table 4 lists all the data for our sample that will be used in the analysis below.

4. Galaxy indices: theory versus data

In this section we compare the observational indices of the galaxies in our sample with those from model calculations.

4.1. The σ , Mg2, Fe diagnostic

In Fig. 2 the velocity dispersion and two iron indices (Fe5270 and Fe5335) are shown as a function of the Mg2 index, separately for the sample of shell-galaxies and pair-members.

Shell-galaxies show a narrower range of values with respect to pair-members. Apparently the shell-sample does not contain low velocity dispersion objects. Furthermore all shell-galaxies lie above the *universal* σ vs. Mg2 relation by Bender et al. (1993). On the contrary, the pair-members nicely follow this relation.

The behavior in the other index-index diagrams is quite similar for the two samples even if they differ in some details. First shell-galaxies tend to have both strong Mg2 and Fe indices at the same time, whereas pair-galaxies have a broader distribution both in Mg2 and Fe indices. Furthermore, in our sample, while the *weak lined* galaxies (i.e. low values of metal indices), pair-members only, are almost consistent with the theoretical prediction, *strong lined* galaxies fall below it. In fact, it has long been known that (e.g. Worthey et al. 1994) the relation between Fe indices and Mg2 tends to be flatter than that traced by the evolutionary path of SSPs. This fact has been interpreted as evidence of enhancement in α elements with respect to the solar partition (perhaps caused by Type II super-novae contamination). We will come back later to this topic.

The peculiar σ vs. Mg2 diagram of shell-galaxies conforms to what is found for field galaxies with the fine structure index Σ of Schweizer (1992) larger than 2 (Bender et al. 1993). However in our sample the effect is more significant.

Among the galaxies showing fine structures, shells are believed to be a signature of past strong dynamical interaction (Barnes 1996). If this mechanism is responsible of the above displacement, several explanations are possi-

Table 4. Basic data for our sample of shell- and pair-galaxies. The velocity dispersion σ is km/s.

Pair-Galaxies								Shell-Galaxies							
Name	H β	Mg2	Mgb	Fe52	Fe53	MgFe	σ	Name	H β	Mg2	Mgb	Fe52	Fe53	MgFe	σ
RR24a	-2.60	0.17	2.49	2.22	2.32	2.90	101	N813	2.29	0.25	4.19	3.33	2.28	4.33	208
RR24b	-17.37	0.09	2.01	0.74	1.10	1.61	92	N1210	1.44	0.26	3.94	2.92	2.46	4.04	180
RR62a	1.15	0.13	2.30	1.57	1.82	2.39	81	N1316	2.01	0.26	4.02	2.84	2.62	4.08	250
RR101a	1.86	0.23	3.53	3.10	2.76	3.98	162	N1549	1.71	0.29	4.46	2.85	2.64	4.31	225
RR101b	2.35	0.23	3.67	2.83	2.35	3.83	210	N1553	1.40	0.30	4.45	3.05	2.79	4.45	188
RR105a	1.32	0.27	4.23	3.21	2.26	4.29	130	N1571	1.66	0.28	4.31	3.24	2.48	4.39	224
RR187b	2.87	0.22	3.40	2.69	2.34	3.62	144	N2865	3.12	0.22	3.28	2.34	2.22	3.36	208
RR210a	0.80	0.33	4.97	2.71	2.47	4.43	281	N2945	0.38	0.26	4.80	2.62	2.21	4.23	212
RR210b	1.50	0.31	4.62	2.99	2.44	4.41	212	N3051	1.15	0.30	4.82	2.74	2.45	4.37	212
RR225a	1.76	0.34	4.96	3.41	2.40	4.78	357	N5018	2.68	0.22	3.31	2.89	2.24	3.64	247
RR225b	1.18	0.31	4.42	2.80	2.59	4.26	186	N6776	1.92	0.25	4.39	2.67	3.15	4.32	243
RR278a	-1.67	0.20	4.14	2.20	2.44	3.76	184	N6849	1.32	0.28	4.34	3.03	2.67	4.35	198
RR282b	1.53	0.33	5.17	2.78	2.16	4.47	290	N6958	1.66	0.26	4.08	2.80	2.29	4.01	223
RR287a	1.61	0.28	4.57	3.08	2.43	4.43	205	E1070040	2.30	0.25	3.97	2.98	2.74	4.16	155
RR297a	1.97	0.27	4.08	2.89	2.32	4.06	177	E3420390	1.32	0.33	4.77	3.15	2.75	4.65	327
RR297b	1.17	0.26	4.81	2.92	2.60	4.51	147	N7135	-0.41	0.31	5.51	2.81	2.38	4.70	191
RR298b	1.42	0.31	4.48	3.24	2.44	4.47	130	E2890150	0.29	0.20	3.06	2.22	2.47	3.25	274
RR307a	0.08	0.21	3.73	1.59	1.53	2.97	92	E2400100a	1.54	0.28	4.63	2.66	2.71	4.31	225
RR317a	1.56	0.28	4.36	3.06	2.90	4.43	189	E2400100b	2.79	0.21	3.79	3.10	2.33	4.02	223
RR317b	2.33	0.13	1.80	2.47	1.74	2.45	91	E5380100	1.70	0.31	4.20	3.01	2.10	4.13	178
RR381a	1.64	0.31	5.01	2.63	2.62	4.44	276								
RR387a	2.20	0.29	4.48	3.08	2.74	4.47	187								
RR387b	1.83	0.31	4.51	3.13	2.55	4.45	215								
RR397b	1.33	0.29	4.39	3.21	2.87	4.52	198								
RR405a	1.45	0.28	4.68	2.92	2.39	4.39	192								
RR405b	1.89	0.34	4.81	2.72	2.76	4.44	207								
RR409a	1.89	0.29	4.51	3.02	3.28	4.59	187								
RR409b	1.17	0.31	4.56	2.89	2.36	4.31	150								

ble: (i) the major effect of dynamical interaction is on the velocity dispersion and other structural quantities rather than on the photometric properties of shell-galaxies; in such a case the object moves vertically away from the universal σ vs. Mg2 relation and maintains its position in the index-index planes. (ii) As suggested by dynamical models of strong unbound encounters, the central velocity dispersion of the interacting objects remains unchanged and the main effect is a burst of star formation altering only the spectro-photometric properties, i.e. displacing them toward *bluer*, *younger* values of Mg2. Most likely a combination of the two effects is at work.

Though far from being statistically complete, we argue that our sample could sketch two consecutive phases of the accretion process: interaction and merging. We note that our selection criteria are biased toward pair-objects obeying the universal σ vs. Mg2 relation.

4.2. On the enhancement of α elements

Assuming that Fe5270 and Mg2 are good indicators of the iron and magnesium abundances Z_{Fe} and Z_{Mg} , respectively, G93 and Worthey et al. (1992) inferred that the [Mg/Fe] ratio changes with the mass of galaxies. Giant galaxies are characterized by a high [Mg/Fe] ratio, whereas ordinary galaxies by a lower, nearly solar ratio.

Several scenarios have been proposed by G93, Worthey (1992), Worthey et al. (1992) to explain the observed Fe vs. Mg2 relation and the inferred over-abundance of Mg passing from ordinary to giant (bright) early-type galaxies

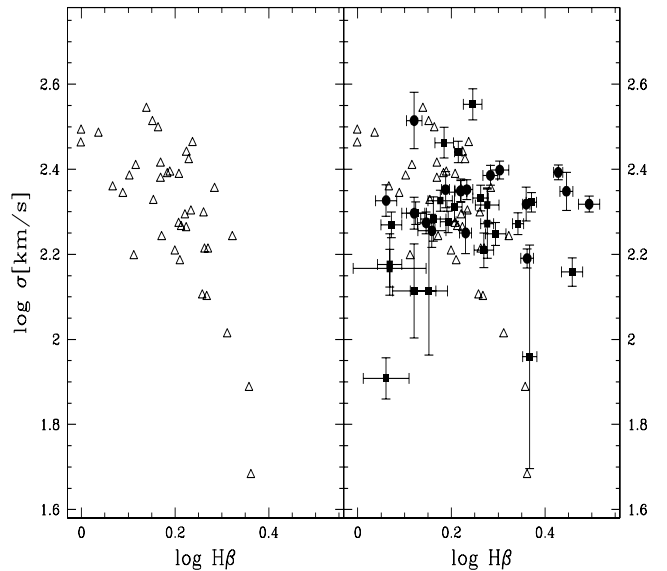


Fig. 3. Left panel: correlation found by G93 between velocity dispersion and H β for a sample of 40 *normal* elliptical galaxies. Right panel: the same but for shell- (full circles) and pair-galaxies (full squares) superposed to the *normal* galaxies by G93. The error bars are also indicated

(see also Matteucci 1997 for a recent review of the subject).

All of these interpretations stand on the notion that heavy elements (like Fe) are predominantly generated by Type I super-novae, whereas lighter elements (like O, Mg,

Si) are produced by Type II super-novae. As Type I and II SNe have progenitors with very different stellar masses (intermediate, low-mass stars the former, and massive stars the latter), the production of O, Mg, Si occurs much earlier than the bulk production of Fe.

The goal is reached by supposing that star formation stops much earlier in giant galaxies than in compact ones. G93's suggestion is somehow supported by the simple interpretation of the distribution of early-type galaxies in his sample on the $H\beta$ vs. $[Mg/Fe]$ plane (see below). Furthermore, considering the velocity dispersion σ as a measure of the galaxy mass, he argued that massive galaxies appear to be older than the low mass ones.

Incidentally, this opposes the standard galactic wind scenario proposed long ago by Larson (1974) to explain the color-magnitude relation of early-type galaxies.

It is worth noting that short-lived star formation in giant (massive) galaxies with respect to that in the compact (less massive) ones is not fully supported by major current theories of galaxy formation. In fact, in the gravitational collapse scenario, star formation in giant elliptical galaxies is expected to last longer than in the compact galaxies, because in the former the dynamical time scale is larger (about 3 times) than in the latter. Conversely, in the hierarchical scenario, where big galaxies are the result of several mergers, global star formation is expected to last for long periods of time. In any case, both scenarios predict giant galaxies to be *younger* than compact galaxies.

To cast light on this intriguing affair, Borges et al. (1995) have recently provided a new empirical calibration of the Mg2 index, that takes explicitly into account the relative abundance of the Mg element. They express the Mg2 index as a function of effective temperature, gravity, $[Fe/H]$ and $[Mg/Fe]$. Tantaló et al. (1998) included the new calibration of Borges et al. (1995) in their models of synthesis of stellar populations, and they calculated the expected integrated Mg2 index for SSPs of various ages and metallicities, assuming the same isochrone for different abundance ratios at a given total metallicity. From their analysis of the G93 sample, younger galaxies seem to be moderately more metal rich and less $[\alpha/Fe]$ enhanced than the older ones (see figures 5 and 6 in Tantaló et al. 1998). The present study adopts the “standard” fitting functions, based on solar abundance ratios, and thus it cannot follow their detailed abundance analysis. Nevertheless, their results will appear to be strengthened when a larger sample of galaxies is analyzed in the $[Mg/Fe]$ vs. $H\beta$ diagram (see next section).

4.3. The σ vs. $H\beta$ diagnostic

According to Worthey (1992) and Bressan et al. (1996) MgI, MgH and FeI indices are good metallicity indicators whereas $H\beta$ is more suited to age determinations.

According to G93, in the case of SSPs, $H\beta$ is a good age indicator as it reflects the temperature of the turn-

off stars. In galaxies, recent experiments with composite stellar populations suggest that $H\beta$ yields a sort of *mean* age of the stellar populations, as it tends to over-weight the age of the young stellar component with respect to the age of the bulk stars (see e.g. Bressan et al. 1996).

The two panels of Fig. 3 make evident the different behavior of our sample (right) and G93 sample (left panel) in the σ vs. $H\beta$ plane. G93 found a correlation between σ and $H\beta$ indicating that *normal* ellipticals, characterized by a shallower gravitational potential, are predominantly young objects as indicated by their high value of $H\beta$ (see also Fig. 11 in Bressan et al. 1996).

In our sample there are a number of galaxies with high σ and $H\beta$ values at the same time. This is particularly true for the sample of shell-galaxies. This finding implies the existence of a family of galaxies with deep gravitational potentials and relatively young ages.

This can be a consequence of the interaction experienced by these galaxies that increases both σ and $H\beta$ (thus making them appear younger).

Rampazzo et al. (1999a) have shown that shell-galaxies seem actually to belong to the family of giant galaxies, as far as their effective radius and surface brightness are concerned (see Fig.2 in Rampazzo et al. 1999a). In contrast, pair-members have a much wider distribution, going from normal to giant galaxies.

Following G93, we would expect that shell-galaxies (high σ and high mass in turn) are old stellar systems, in which the young component formed during a recent interaction and/or merger episode is either too old or too weak to be able to affect the global Mg indices. The fact that the *strong lined* pair-members show the same behavior of shell-galaxies (i.e. deviation from the Fe vs. Mg2 relation and likely high $[Mg/Fe]$ ratios) whereas the *weak-lined* ones agree with the above relation and likely have *normal* $[Mg/Fe]$ ratio, leads us to argue that a much larger spread in age ought to exist among pair-members as compared to shell-galaxies. Checking this point requires the use of $H\beta$ as age indicator (see below).

As our sample is composed of objects in interaction and/or post-interaction stages, the mean age of their stellar populations is less meaningful with respect to that of the *normal* ellipticals of G93. In fact, an old age for the *giant* galaxies does not exclude the possible presence of a young component formed in a recent (or ongoing) event involving only a small percentage of the total mass of the galaxy.

4.4. $H\beta$ vs. $[Mg/Fe]$ diagnostic

Fig. 4 presents the shell- and pair-galaxies of our sample (dots and squares, respectively) in the $[Mg/Fe]$ - $H\beta$ plane and compares them with theoretical models.

Three SSPs (dashed lines) with different chemical composition, i.e. $[Y=0.250 Z=0.004]$, $[Y=0.280 Z=0.020]$ and $[Y=0.0.335 Z=0.05]$, are plotted as a function of the

age, and lines of constant age are also indicated (dotted-dashed).

In the same diagram we plot the G93 galaxies (asterisks) and the mean value for the early-type galaxies of the Virgo cluster (large open circle). The two sets of data share the same properties but differ in some important aspects. Pair- and shell-galaxies show a global metallicity similar to that of the *normal* G93 galaxies, and no difference between the shell-galaxies and pair-members appears in this diagram. At the same time we notice that the $H\beta$ values for our sample extend up to the top of the $[MgFe] - H\beta$ plane, where *normal* galaxies are not found.

There is a group of galaxies whose $H\beta$ is much lower than predicted by models of old age (say 15 Gyr). These galaxies are likely to have $H\beta$ affected by contamination of the $H\beta$ emission line whose net effect is to decrease the value of $H\beta$ by partially filling up the corresponding absorption feature.

The last thing to note is that the distribution of galaxies in this plane, of shell- and pair-objects in particular, is significantly steeper than the path followed by SSPs. The locus of real galaxies stretches almost vertically along the $H\beta$ axis and covers a narrow range of $[MgFe]$.

5. Individual galaxies on the $H\beta$ vs. $[MgFe]$ plane

This section is dedicated to discussing in some detail the location of groups of galaxies on the $H\beta - [MgFe]$ plane trying firstly to understand the reason of their position and secondly to decipher the underlying age. Particular attention is paid to some of the galaxies in the sample, the shell-galaxies in particular. In fact for a few of them independent estimates of the age of the last burst of star formation based on morphological observations and dynamical models can be found in the literature. Consistency between photometric and dynamical age estimates would provide useful insight on the connection between dynamical processes and star formation.

5.1. Galaxies showing emission lines

Some of the galaxies of our sample show clear emission lines. In particular, among the pair galaxies, we find a detectable $[OII](3727\text{\AA})$ line in 10 objects (in RR278a this line can be detected but its measure is very uncertain for the high noise of the corresponding spectrum around 3700\AA). A subsample of 3 out of 10 galaxies (RR24a, RR24b and RR278a) shows also the $[OIII](5007\text{\AA})$ line and the $H\beta$ emission. Among shell galaxies, the $[OII](3727\text{\AA})$ line can be detected in 7 objects 4 of which (NGC 7135, NGC 1210, NGC 6958 and NGC 2945) show also the $[OIII](5007\text{\AA})$ line, whereas the $H\beta$ emission can be detected (even if measured with great uncertainty) only in NGC 7135.

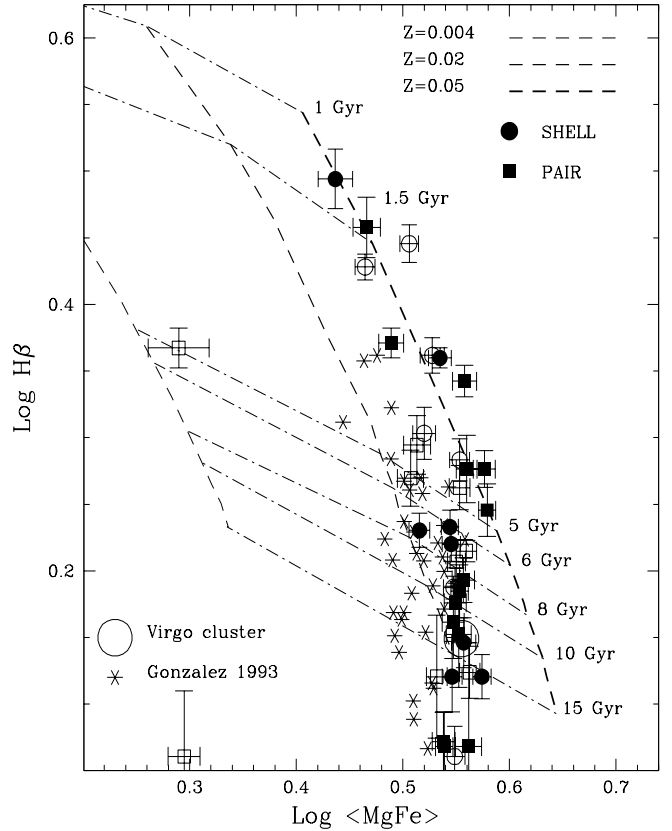


Fig. 4. The position of shell- (filled dots) and pair-galaxies (filled squares) together with their 1σ error bars onto the $[MgFe] - H\beta$ plane. Open circles and squares indicate shell galaxies and pair galaxies (respectively) showing emission lines. The asterisks indicate the *normal* elliptical galaxies by G93, for purposes of comparison. The large open circle is the average value for the 7 galaxies in the G93 sample members of the Virgo. Superposed to the data are the evolutionary paths (dashed lines) of SSPs with different metallicity as indicated. The models go from the age of 1.0 (top) to 15 Gyr (bottom). Lines of constant age are also shown (dotted-dashed lines)

In Fig. 4 the four galaxies (3 pair objects and 1 shell galaxy) showing $H\beta$ in emission are not shown (their $H\beta$ index being negative).

As far as the remaining galaxies with measured $[OIII](5007\text{\AA})$ emission (NGC 1210, NGC 6958 and NGC 2945) are concerned, adopting the G93 correction they would shift by $\delta\text{Log}H\beta = +0.27, +0.67$ and $+3.4$, respectively.

Given the high expected correction we have decided not to display these galaxies in Fig. 4.

For the galaxies showing only $[OII](3727\text{\AA})$ line in emission (3 shell galaxies and 7 pair members), we used open symbols, in order to stress that the value of the $H\beta$ index can be affected by the emission contamination. However, by considering that the threshold of $[OIII](5007\text{\AA})$

detection in our spectra is about 0.1\AA , we estimate that in these latter galaxies the correction to the observed $\text{Log}(H\beta)$ is less than $+0.15$ dex.

As previously pointed out, no correction for emission has been applied to the values of $H\beta$ shown in Fig. 4.

5.2. Galaxies with low $[\text{MgFe}]$ values

RR 317b and RR 62a have unusually low values of $[\text{MgFe}]$ and very different values of $H\beta$, very high in RR 317b and very low in RR 62a. Furthermore, while RR 317b shows evidence of emission $[\text{OII}](3727\text{\AA})$, no detection is found in RR 62a (Longhetti et al. 1998b). Rampazzo et al. (1999a) have shown that in the $\mu_e - R_e$ plane both galaxies occupy the same area as *ordinary* galaxies. In addition to this, RR 62a lies outside the Hamabe-Kormendy (1987) relation which holds for bright galaxies. All this implies that both galaxies are not giant objects. According to Gorgas et al. (1993) dwarf galaxies populate the left part of the $H\beta - [\text{MgFe}]$ plane showing a metallicity lower than in giant ellipticals. In this context, the location of RR 62a and RR 317b can be explained.

5.3. Galaxies with high $H\beta$ values

Bressan et al. (1996) investigated the evolutionary path in the $H\beta$ vs. $[\text{MgFe}]$ plane of a galaxy in which a recent burst of star formation is superposed to a much older population.

As soon as the burst begins, the galaxy runs away from the locus of quiescence toward the top of the $H\beta - [\text{MgFe}]$ plane following a nearly vertical path. As soon as the burst is over, on a short time scale, the galaxy goes back toward its original position sliding along a path that is also nearly vertical. A loop is performed. See the numerical experiment described by Bressan et al. (1996), in which a burst with 1% of the galaxy mass engaged in the star forming activity and duration of 10^8 years is calculated and displayed in the $H\beta$ vs. $[\text{MgFe}]$ plane (Figs. 7 & 8 in Bressan et al. 1996). Since the burst intensity and duration may vary from one case to another, a large variety of loops are possible in the $H\beta$ vs. $[\text{MgFe}]$ plane. Stronger and longer bursts induce wider loops and longer recovery time scales.

Looking at post-star-burst objects such as the shell-galaxies, they are expected to closely follow the distribution of star-burster simulations and to somehow depart from the region occupied by the *normal* galaxies of G93. This could be the case for galaxies with very high values of $H\beta$ ($\text{Log}H\beta > 0.35$) present in our sample, namely NGC 813, NGC 2865, NGC 5018, ESO 2400100b, ESO 1070040, RR 187b, RR101b. None of these galaxies show emission lines in their spectra, apart from ESO 2400100b that shows only the $[\text{OII}](3727\text{\AA})$ line. With lower $H\beta$ ($0.25 < \text{Log}H\beta < 0.35$), but different position with respect to the G93 sample, there are also NGC 1316, NGC 6776 (with $[\text{OII}](3727\text{\AA})$ emission de-

tected in their spectra), RR 225a, RR 387b RR 409a, RR297a, RR101a and RR 405b.

Pair-members. None of the pair-members in this area show emission lines in the spectrum, apart from RR101a that shows the $[\text{OII}](3727\text{\AA})$ line. All systems they belong to show signs of interaction at least in one of the members. From the morphological signatures and the absence of emission lines we suggest that these pairs have already passed through the strongest interaction phase and are now recovering from a burst that likely occurred less than 1 Gyr ago.

ESO 2400100. Longhetti et al. (1998a) showed that ESO 2400100 is actually made up of two components separated by $5''$ and 200 km s^{-1} . This feature is present in three independent spectra. Probably what we are seeing is an ongoing merger accompanied by star formation as suggested by the very high value of $H\beta$. The component ESO 2400100a falls, however, in the area of *normal* galaxies.

NGC 2865. This shell-galaxy is at the top of the $[\text{MgFe}]$ vs. $H\beta$ plane. Our data, interpreted at the light of Bressan et al. (1996) simulations, suggest that a burst of star formation has occurred very recently, probably less than 1 Gyr ago. This galaxy has been observed by Schiminovich et al. (1995), who derive from VLA images, a correlation between the HI distribution and the fine structures (shells, tails, and loops) hosted by the galaxy. The authors argue that the lack of HI gas in the center could be explained by a burst of star formation. The origin of the shells and the evolution of NGC 2865 remain in any case unclear. The question to be asked is why the $[\text{MgFe}] - H\beta$ plane hints at a recent burst, while the correlation between shells and stellar motions favors ≈ 7 Gyr old merger.

NGC 1316. The position of this galaxy in the $H\beta$ vs. $[\text{MgFe}]$ diagram suggests that it has undergone a recent burst of star formation. Very recently, Mackie & Fabbiano (1998) studied the evolution of gas and stars in the optical and X-ray bands. They emphasized the presence in NGC 1316 of a complex tidal-tail system, that hampers the accurate reconstruction of its past history (mergers). Speculating about some observational indications which hint at an efficient conversion of HI into other gas phases, Mackie & Fabbiano (1998) suggest that a low-mass, gas-rich galaxy could have started merging ≈ 0.5 Gyr ago. A longer time scale is proposed by Schweizer (1980) to explain NGC 1316 as the product of several mergers of gas-rich galaxies over the past ≈ 2 Gyr.

5.4. Galaxies with normal $[\text{MgFe}]$ and $H\beta$ values

In the area occupied by the majority of the G93 galaxies, in particular those which are members of the Virgo cluster, we find both shell-galaxies and pair-members. The age of the bulk stellar population in these galaxies can be estimated as old as 10-15 Gyr. If a star-burst phenomenon has ever occurred, its signatures on the stellar popula-

tions of the galaxies located in this area of the diagram have already faded away. Shell-galaxies falling in this region (NGC 1549, NGC 1553, IC 5105, NGC 6849) suggest that shells are long-lasting morphological features, which can be detected also after star formation signatures have disappeared.

6. More on the $H\beta$ vs. $[Mg/Fe]$ plane

Starting from the idea of Bressan et al. (1996) that the distribution of galaxies in the $H\beta$ vs. $[Mg/Fe]$ plane may reflect secondary episodes of star formation superposed to an old stellar component, we present here the results of simulations designed to clarify this point. In the analysis below, we will neglect any effects due to $[\alpha/Fe]$. As a matter of fact, first no calibration accounting for different $[Mg/Fe]$ ratios is available for the Mgb index (in analogy to that of Borges et al. (1995) for the Mg2 index). Furthermore, any increase in the $[Mg/Fe]$ is expected to be associated with a decrease in $[Fe/H]$, and the two effects likely parallel each other in final determination of $[Mg/Fe]$. Therefore, $[Mg/Fe]$ can be safely considered as a good, global indicator of metallicity (see also G93).

We have constructed models aimed at predicting the statistical distribution of 80 post-burst galaxies, and to reproduce the observational one displayed in Fig. 4. Following the selection criteria explained in the previous section, the observational sample to be matched is composed of about 20 shell galaxies, 20 pair members and 40 “normal” galaxies from G93.

We simplify the complex star formation history of an early-type galaxy to a bulk population made of old stars on which a more recent burst of activity with different age and intensity is superposed. The old stars are in turn represented by a SSP whose age is randomly chosen between T_1 and T_2 , parameters in the models. We are aware that this oversimplified scheme neglects the complex star formation histories of real galaxies and the ensuing mixture of stars with different chemical composition.

Integrated indices of SSPs, resulting from multi-population models, have been investigated by Idiart et al. (1996) and Bressan et al. (1996). In particular, the complex chemical modeling used by Bressan et al. (1996) suggests that field early-type galaxies are confined within a narrow range of metallicities, around the mean value. For the sake of simplicity, we will use the mean metallicity (despite the physical process by which galaxies get enriched in metals, e.g. closed-box, infall, etc.) to rank galaxies as a function of this parameter.

The young stellar component, formed during the recent burst of star formation, is represented by a SSP whose age is randomly varied between 0.1 Gyr and T_3 . The value of T_3 has been fixed to 1 Gyr for 20 models in order to represent the 20 pair members. These latter in fact seem to be characterized by a very young stellar component gen-

erated by the ongoing dynamical interaction (Longhetti et al. 1999).

For the remaining 60 objects, T_3 is allowed to arbitrarily vary from young to old ages (up to T_2). The strength of the secondary burst, represented by the percentage of the total mass turned into stars, is randomly chosen between 0 (no secondary stellar activity) and f , a parameter of the models. Since we are interested in guessing the minimum threshold above which the secondary episode has a sizable effect on the line strength indices, we will consider only the case in which the secondary episode involves a minor fraction of the galaxy mass.

The metallicity Z of both stellar components is randomly varied from $Z=0.015$ (75% of the solar value) to $Z=0.025$ (1.25 the solar value). We have also calculated a set of simulations in which the metallicity is supposed to linearly increase from $Z=0.015$ to $Z=0.04$ (twice the solar value) over the time interval T_1-T_2 .

Finally, random errors $\Delta\text{Log}([Mg/Fe]) \leq 0.011$ and $\Delta\text{Log}(H\beta) \leq 0.02$ are applied to the model indices to better simulate observational data.

In Fig. 5 we show an example of the 80 simulated galaxies for 4 different models. The aim is to highlight the effects of the underlying basic parameters, namely the epoch at which the bulk stars have been formed, the strength of the more recent burst episode, if any, and its age.

In panels (a) and (b) galaxies are conceived as old, nearly coeval systems, their population being approximated by a single SSP with age between 14 and 16 Gyr; this corresponds to the current view of elliptical galaxies in rich clusters (Bower et al. 1998). The maximum intensity of the superposed burst amounts to 10% and 2% of the total mass, panels (a) and (b) respectively.

Inspection of the results shown in panel (a) indicates that model galaxies with a burst engaging a percentage of the total mass up to 10% predicts too high values of $H\beta$ and too many *young* objects. In contrast, the models of panel (b) span the range of $H\beta$ values indicated by the observations. In both cases, however, the expected distribution of objects with respect to the $H\beta$ index is at variance with the observational one. Indeed models of this type predict a bimodal distribution, whereby the old galaxies (those for which the burst is almost as old as the bulk of their stellar populations) clump together in the lower portion of the diagram, whereas the “young” objects (those with very young bursts) form a tail extending to high values of $H\beta$. The real clump is even narrower than displayed if one considers the effect of the simulated errors.

The tail of “young” models agrees quite well with the observations, thus suggesting that the upper part of the diagram is populated by objects which experienced a recent burst of star formation of minor entity (less than 2% of the total mass).

The burst alone cannot, however, explain the smooth distribution observed at low values of $H\beta$. The reason for

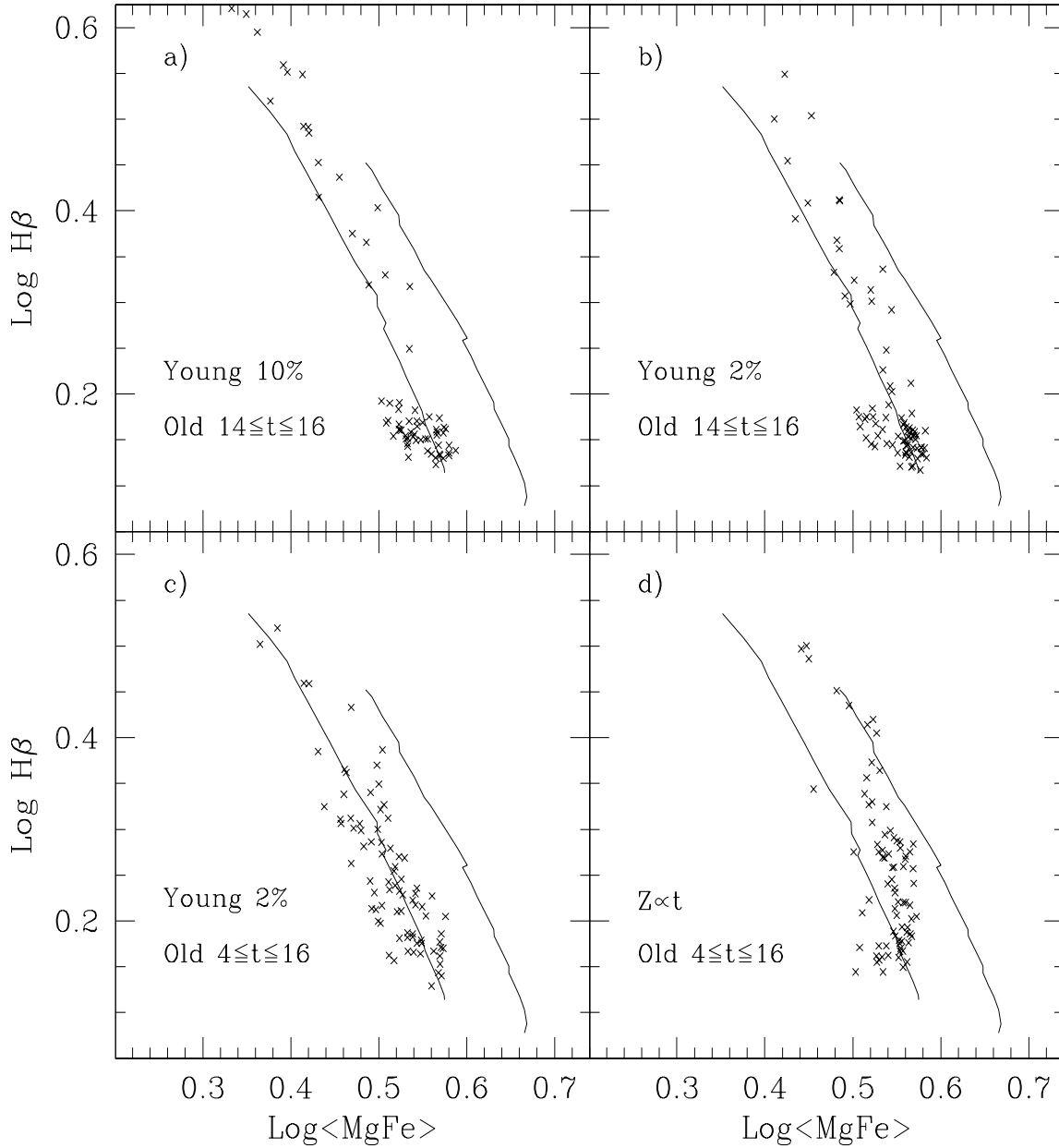


Fig. 5. Simulations of 80 galaxies in the $H\beta$ vs. $[MgFe]$ plane. The age of the burst is randomly chosen between 0.1 Gyr and 1 Gyr for 20 galaxies (simulated pair-members) and the bulk age for all remaining objects (60 in total). The fraction of the mass stored in the young component is randomly chosen from zero to either 10% -panel (a)- or 2% -panels (b), (c) and (d)-. The age of the bulk (old) component is randomly fixed between the values indicated in the corresponding panels. In panels (a), (b) and (c) the metallicity is allowed to randomly vary from $Z=0.015$ to $Z=0.025$. In panel (d) the metallicity is allowed to linearly increase with age from $Z=0.015$ to $Z=0.04$. Random errors $\Delta\text{Log}([MgFe]) \leq 0.011$ and $\Delta\text{Log}(H\beta) \leq 0.02$ are applied to model indices to better simulate the data. Finally, the solid lines are two SSPs with $Z=0.02$ (left) and $Z=0.05$ (right).

it is that the index $H\beta$ of a composite stellar population (2% of the mass is “young” stars and the remaining 98% in old stars), soon after the maximum excursion toward high values of $H\beta$, fades out very rapidly as the young population ages. Therefore catching a galaxy at intermediate values is highly improbable.

Slowing down the evolutionary rate of the “young” component by increasing the percentage of mass involved in the young burst produces an uncomfortably large fraction of objects in the upper part of the diagram, e.g. panel (a).

Since a sort of fine tuning between the old and young component is not easy to understand, the viable alternative is that the old component spreads over significantly longer periods than assumed in the above simulations. To this aim, we present the models shown in panels (c) and (d). The *old* population in these models has an average age that spreads over a significant fraction of the Hubble time. This is meant to indicate that either the object has been growing for such a long time with a low star formation rate, or that its major star formation activity was not confined to an early epoch. The young component is allowed to occur as in the simulations of panel (b). It is immediately evident that the new models much better reproduce the distribution of galaxies all over the range of $H\beta$.

However, problems remain if the metallicity is randomly chosen. Indeed, the model galaxies always tend to follow the path of an SSP, in these simulations the SSP with $Z=0.02$ as shown in panel (c). As already anticipated, real galaxies seem to follow a path steeper than that of SSP. We consider this point as evidence of an underlying relation between the age and metallicity of the bulk population of stars. Panel (d) shows our final experiments, where the average metallicity of the bulk stars has been supposed to linearly increase with age from $Z=0.015$ to $Z=0.04$. The broad range of metallicity is required by the large scatter in $\text{Log}([\text{Mg}/\text{Fe}])$. If this suggestion is sounded, it would imply that young early type galaxies in the field are on average more metal-rich than old systems, with an average rate of metal-enrichment $\Delta\text{Log}(Z)/\Delta\text{Log}(t)\simeq-0.7$. If confirmed, the vertical distribution of galaxies in this diagram is therefore *the trace of a global metal enrichment taking place in galaxies during all the star forming episodes*.

7. Summary and conclusions

In this paper firstly we have compared the line strength indices for SSPs that one would obtain using different calibrations in literature, namely Worthey (1992), Worthey et al. (1994), Buzzoni et al. (1992, 1994) and Idiart et al. (1995). Secondly, with the aid of the Worthey (1992) and Worthey et al. (1994) calibrations, the sample of shell- and pair-galaxies by Longhetti et al. (1998a,b), and the sample of G93 for *normal* elliptical galaxies have been systemati-

cally analyzed, looking at the position of all these galaxies in various diagnostic planes. The aim is to cast light on the star formation history that took place in these systems with particular attention to those (shell- and pair-objects) for which the occurrence of dynamical interaction is evident. Finally, from comparing normal to dynamically interacting galaxies we attempt to understand the reasons for their similarities and differences.

The results of this study can be summarized as follows:

(1) The various calibrations for the line strength indices as a function of basic stellar parameters (effective temperature, gravity and metallicity) lead to quite different results. Specifically, the Buzzoni et al. (1992, 1994) calibrations for Mg2 and Fe5270 agree with those by Worthey (1992) and Worthey et al. (1994) only for SSPs older than 3 Gyr. For $H\beta$ the agreement is also good if one excludes all ages younger than about 1 Gyr. Idiart’s et al. (1995) calibrations can be compared with the others only for a limited range of SSP ages. For the Mgb and Mg2 indices we find a roughly constant offset, that could be attributed to different properties (g.e., metallicity, gravity) of the calibrating sample of stars. For the purposes of this study we have adopted Worthey (1992) and Worthey et al. (1994) as the reference calibrations.

(2) The comparison of the Mg and Fe indices (specifically Mg2, Fe5270 and Fe5335) and the velocity dispersion σ of normal, shell- and pair-galaxies suggests firstly a different behavior of shell-galaxies with respect to pair-objects and secondly that strong-lined galaxies are likely to have super-solar $[\text{Mg}/\text{Fe}]$ abundance ratios. Various kinds of star formation histories leading to super-solar $[\text{Mg}/\text{Fe}]$ are examined at the light of current understanding of the mechanisms of galaxy formation. None of these is however able to give a self-consistent explanation of the $[\alpha]$ -enhancement problem.

(3) The same galaxies are analyzed in the $H\beta$ vs. $[\text{Mg}/\text{Fe}]$ plane and compared to the G93 set of data. The shell- and pair-objects have the same distribution in this diagnostic plane as the *normal* galaxies even if they show a more pronounced tail toward high $H\beta$ values.

(4) The $H\beta$ vs. $[\text{Mg}/\text{Fe}]$ plane is divided in several sub-regions carefully inspected in order to look for all plausible causes that would justify the positions of the galaxies.

(5) As shell- and pair-galaxies share the same region of the $H\beta$ vs. $[\text{Mg}/\text{Fe}]$ plane occupied by *normal* galaxies, we suggest that a common physical cause is at the origin of their distribution. The star formation history in these objects is investigated with the aid of very simple galaxy models.

We find that the tail at high $H\beta$ values can be ascribed to secondary bursts of star formation which, in the case of shell- and pair-galaxies, can be easily attributed to interaction/acquisition events whose signatures are well evident in their morphology.

(6) A typical model where the burst is superimposed to an otherwise old and coeval population is however not

able to reproduce the smooth distribution of galaxies in the $H\beta$ vs. $[MgFe]$ plane. This kind of model would predict an outstanding clump at low $H\beta$ values, contrary to what is observed. Models in which the bulk of the star formation happened over a significant fraction of the Hubble time ($4 \text{ Gyr} \leq t_{old} \leq 16 \text{ Gyr}$) better match the observed diagram.

(7) In this context, the peculiar, smooth and almost vertical distribution of galaxies (normal, shell-pair-objects) in the $H\beta$ vs. $[MgFe]$ plane is interpreted as the trace of the increase of the average metallicity accompanying all star forming events. This could be the signature of a metal enrichment happening on a cosmic scale.

(8) Although deciphering the position of galaxies in the $H\beta$ vs $[MgFe]$ plane to infer the age of the constituent stellar populations is a difficult task due to possible blurring caused by the secondary stellar activity, still we may draw some conclusions for the duration of the shell phenomenon. Specifically, since shell-galaxies can be found in the same region of old normal galaxies, we may say that shells are a morphological feature able to persist for long periods of time, much longer than the star forming activity that likely accompanied their formation. Among current dynamical models in which shell-structures can be formed, the *weak interaction* mechanism of Thomson & Wright (1990) and Thomson (1991) naturally predicts long-lived shells without particular hypotheses on the type of encounters.

Acknowledgements. ML acknowledges the kind hospitality of the Astronomical Observatory of Brera (Milan) and Padua during her PhD thesis and the support by the European Community under TMR grant ERBFMBI-CT97-2804. CC wishes to acknowledge the friendly hospitality and stimulating environment provide by MPA in Garching where this paper has been completed during leave of absence from the Astronomy Department of the Padua University. This study has been financially supported by the European Community under TMR grant ERBFMRX-CT96-0086.

References

- Barnes, J.E. & Hernquist, L.E. 1992, ARA&A 30, 705
 Barnes J., 1996, in *Galaxies: interactions and induced star formation*, Saas-Fee Advances Course 26,275.
 Bender, R., Burstein, D. & Faber, S.M. 1993, ApJ 411, 153
 Bender R. 1997, *The Second Stromlo Symposium: The Nature of Elliptical Galaxies*, Ed.s M. Arnaboldi et al., p 11
 Bertelli G., Bressan A., Chiosi C., Fagotto F., Nasi E., 1994, A&AS 106, 275
 Borges, A.C., Idiart, T.P., de Freitas Pacheco, J.A. & Thevenin, F. 1995, AJ 110, 2408
 Bower, R.G., Ellis, R.S., Rose, J.A. & Sharples, R.M. 1990, AJ, 99, 530
 Bower, R.G., Tadayuki, K., Terlevich, A. 1998, MNRAS 299, 1193
 Bressan, A., Chiosi, C., Fagotto, F. 1994, ApJS, 94, 63
 Bressan, A., Chiosi, C., Tantalo, R. 1996, A&A, 311, 425
 Burstein, D., Faber, S.M., Gaskell, C.M. & Krumm, N. 1984, ApJ., 287, 586
 Buzzoni, A. Gariboldi, G., Mantegazza, L. 1992, AJ, 103, 1814
 Buzzoni, A. Mantegazza, L., Gariboldi, G. 1994, AJ, 107, 513
 Ellis, R. 1998, Nature, Supplement V. 351, n. 6701, p. A3
 de Jong R.S. and Davies R.L. 1997, M.N.R.A.S. 285, L1.
 Faber, S.M., Friel, E.D., Burstein, D., Gaskell, C.M. 1985, ApJS, 57,711
 Fluks, M.A., Plez, B., The, P.S., DeWinter, D., Westerlund, B.E., Steenman, H.C. 1994, A&AS, 105, 311
 González, J.J. 1993, Ph.D. Thesis, University of California, Santa Cruz: G93
 Gorgas, J., Faber, S.M., Burstein, D., González, J.J., Courteau, S., Prosser, C. 1993, ApJS, 86, 153
 Griffith, M.R., Wright, A.E., Burke, B.F. & Ekers, R.D. 1994, ApJS 91, 111
 Hamabe M. and Kormendy J. 1987, in *Structure and Dynamics of Elliptical Galaxies*, IAU Symp. No. 127 (Princeton), ed. T. de Zeeuw, Dordrecht: Reidel, p. 379: HK87.
 Idiart, T.P., Pacheco, J.A. DeFreitas 1995, AJ, 109, 2218
 Kurucz, R.L. 1992, in *Stellar Populations of Galaxies*, eds. Barbuy, B., Renzini, A: Kluwer Academic Publishers
 Lancon, A., Rocca-Volmerange, B. 1992, A&AS, 96, 593.
 Larson R.B., 1974, MNRAS 166, 585
 Leonardi, A.J., Rose, J.A. 1996, AJ, 111, 182
 Longhetti M., Rampazzo R., Bressan A. and Chiosi C. 1998a, A&AS, 130, 251
 Longhetti M., Rampazzo R., Bressan A. and Chiosi C. 1998b, A&AS, 130, 267
 Longhetti M., Bressan A., Chiosi C. & Rampazzo R. 1999, A&A, 345, 419
 Mackie, G. & Fabiano, G. 1998, AJ, 115, 514.
 Matteucci F. 1997, Fund. Cosmic Phys. 17, 283
 Moore, B., Katz, N., Lake, G., Dressler, A. & Oemler, A. 1996, Nature 379, 613
 Pickles, A.J. 1985, ApJ, 296, 340
 Rampazzo R., D'Onofrio M., Bonfanti P., Longhetti M. and Reduzzi L. 1999a, *Astrophys. Lett. & Comm.*, in press
 Rampazzo R., D'Onofrio M., Bonfanti P., Longhetti M. and Reduzzi L. 1999b, A&A, 341, 357
 Reduzzi, L. & Rampazzo, R. 1996, MNRAS, 116, 515
 Reduzzi, L., Longhetti, M. & Rampazzo, R. 1996, MNRAS, 282, 149
 Rose J.A. 1984, AJ, 89, 1238
 Rose J.A. 1985, AJ, 90, 1927
 Rose J.A. 1995, in *Fresh Views of Elliptical Galaxies*, eds. Buzzoni, A., Renzini, A. & Serrano, A., A.S.P.C. Conf. Series., Vol. 86, p. 157
 Schweizer, F. 1980, ApJ, 237, 303
 Schweizer, F. 1992 in *Structure, Dynamics and Chemical Evolution of Elliptical Galaxies*, ed.s I.J. Danziger, W.W. Zeiliger and K.Kjär, ESO/IPC, p.651.
 Schweizer, F. & Seitzer, P. 1992, AJ, 104, 1039.
 Schiminovich, D., Van Gorkom, J.H., Van der Hulst, J.M. & Malin, D.F. 1995, ApJ, 444, 77
 Straizys, V., Sviderskiene, Z. 1972, Bull. Vilnius Obs, 35, 3
 Tantalo R., Chiosi C., Bressan A., & Fagotto, F. 1996, A&A 311, 361
 Tantalo R., Chiosi C., Bressan A., Marigo P., Portinari L., 1998, A&A 335, 823
 Thomson, R.C. 1991, MNRAS, 253, 256
 Thomson, R.C. & Wright, A.E. 1990, MNRAS, 224, 81B
 Weil, M.L. & Hernquist, L. 1993, ApJ, 405, 142

- Worthey, G. 1992, Ph.D. Thesis, University of California, Santa Cruz
- Worthey, G. 1994, ApJS, 95, 107
- Worthey, G., Faber, S.M. & González, J.J. 1992, ApJ, 398, 69
- Worthey, G., Faber, S.M., González, J.J. & Burstein, D. 1994, ApJS 94, 687